Solvent Effects on Optical Rotation: On the Balance Between Hydrogen Bonding and Shifts in Dihedral Angles

Shokouh Haghdani, Bård Helge Hoff, Henrik Koch,* and Per-Olof Åstrand*

Department of Chemistry, Norwegian University of Science and Technology (NTNU), N-7491 Trondheim, Norway

E-mail: henrik.koch@ntnu.no; per-olof.aastrand@ntnu.no

Abstract

Optical rotations of several conformers of four fluorinated molecules containing the 1-naphthalene or 4-(benzyloxy)phenyl group at the stereocenter have been calculated in both the gas phase and in an aqueous environment. For the compounds containing the 4-(benzyloxy)phenyl group, solvent effects on the optical rotations have also been investigated in chloroform as solvent. Optical rotations have been obtained by time-dependent density functional theory (TDDFT) with the CAM-B3LYP functional and the aug-cc-pVDZ basis set at $\lambda = 589$ nm. Implicit and explicit solvent effects were investigated through the polarizable continuum model (PCM) and a microsolvation approach in conjunction with PCM, respectively. In the latter model, solvent molecules are considered as an explicit solvent and their positions are obtained by geometry optimizations for different conformers of the chiral molecule. For molecules containing the 1-naphthalene group, this model gives the same optical rotation signs for all conformers as compared to both gas phase and PCM results and reduces absolute deviations between calculations and experiment. Also, the microsolvation model reproduces the sign of the experimental optical rotations for the molecules containing the 4-(benzyloxy)phenyl group using both water and chloroform as solvent. In a microsolvation model, however, the water and chloroform solvent molecules have similar hydrogen bonds but different effects on the conformation and thereby on the optical rotation since one dihedral angle, having a large effect on the optical rotation, is strongly sensitive to hydrogen bonding to water but not to chloroform. Our investigations demonstrate that a microsolvation approach in conjunction with PCM predicts optical rotations in reasonable agreements with experiments for both sign and magnitude.

1. Introduction

Chiral molecules are of fundamental importance in many fields of science.[1–9] The determination of their absolute configuration, in the context of synthesis or isolation is crucial for understanding their structure-property relationships. For a new chiral molecule, the determination of its absolute configuration (AC) requires experimental methods such as synthesis from known precursors, X-ray crystallography[10] or chemical correlation. While experimental methods are rather time-consuming and expensive,[11] employing a combination of theoretical and experimental methods has been demonstrated as a valuable tool for predicting the AC by the comparison of a measured optical response of a chiral candidate with theoretical predictions of a known AC.[12–16] This approach has motivated developments of quantum chemical methods to predict chiroptical responses, in particular the optical rotation. Hartree-Fock (HF) theory was introduced as the first quantum chemical method for predicting optical rotation.[17–23] However, density functional theory (DFT)[24–40] and coupled-cluster (CC)[28,31,34,35,37–48] approaches have been used extensively to account for electron correlation and therefore give more accurate predictions.

Since most optical rotation measurements are in the condensed phase (i.e., solutions or pure liquids), a direct comparison between experimental and computational data requires accounting for solvent effects which can change both sign and value of the optical rotations.[49] In this context, the polarizable continuum model (PCM)[50–53] has been shown as an efficient and reliable technique to model bulk solvent effects where specific solute-solvent interactions can be neglected.[54,55] On the other hand, microsolvation models have been employed to explicitly describe specific solute-solvent interactions (short-range solvation effects), such as hydrogen bonding for polar molecules in an aqueous environment, by performing quantum chemical calculations on clusters.[56–62] The solvation clusters consist of a chiral solute molecule surrounded by a few solvent molecules to describe the most important intermolecular interactions where the geometries may be obtained either at the quantum mechanical level by a geometry optimization or by sampling configurations from molecular dynamics

simulations.[56–62]

In our previous work on optical rotation of a set of 45 fluorinated molecules in the gas phase, we found large absolute deviations and opposite optical rotation signs between theoretical and experimental results for the most stable conformers of some molecules containing the 1-naphthalene group as well as for molecules with the 4-(benzyloxy)phenyl group attached to the stereocenter.[40] Therefore, we here study solvent effects on the optical rotation of several conformers for two representative molecules of each category. While the experimental data were reported in ethanol for molecules containing the 1-naphthalene group,[63,66] we choose water molecules as an explicit solvent because of their small size, but still with the possibility to model hydrogen bonds between the solute and the solvent molecules. For molecules containing the 4-(benzyloxy)phenyl group, we investigate solvent effects on the optical rotations using both water and chloroform molecules where the latter was used in the experiments.[64,65] The calculations were performed at the DFT level using the CAM-B3LYP functional[67] and the aug-cc-pVDZ basis set[68–71] based on our previous validation study[38] to include both implicit (employing PCM) and explicit solvent effects on the optical rotations. The CAM-B3LYP functional has been proven as a reasonable choice for calculating excitation energies[72] and optical rotations[37,38,73,74] because of the long-range correction term included in this functional.

This paper is organized as follows: In section 2, the computational details are described. In section 3, the optical rotation results are discussed and compared with experiments for each molecule separately. Finally, we conclude our investigations in section 4.

2. Computational Methods

In this paper, we study the optical rotations of several conformers of the chiral molecules **1**−**4**, shown in Figure 1, in both the gas phase and in solution. All optical rotations were calculated using time-dependent density functional theory (TDDFT)[75–77] with the long-range corrected

CAM-B3LYP functional[67] and the augmented double-zeta basis set, aug-cc-pVDZ,[68–71] as implemented in Gaussian 09.[78] Origin-independent results are obtained by using gauge-including atomic orbitals (GIAOs)[79–81] at the wavelength of the sodium D line i.e. $\lambda = 589$ nm at which the experimental data were measured.[63–66] The method employed has been demonstrated to be an efficient and reliable approach for predicting optical rotations by comparison to the coupled cluster singles-doubles (CCSD) method[82] in a previous work by us.[38]

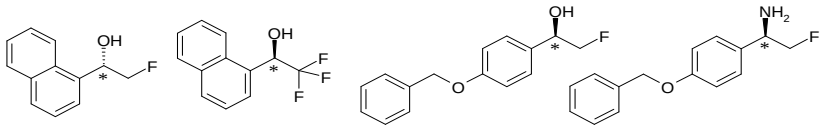

(*S*)-**1** (*R*)-**2** (*R*)-**3** (*R*)-**4**

Figure 1: The structures of molecules **1**−**4**. Chiral centers are denoted by " ∗ ".

The effect of the solvent on the optical rotations were investigated in the implicit model through the integral equation formalism version of PCM (IEFPCM)[50,51] and a microsolvation model with explicit water molecules. In the latter case, PCM was also employed to include the remaining part of the solvent effect. We modeled possible hydrogen bonds between solute and solvent molecules by adding water molecules close to each polar group in the chiral molecule. One water molecule was placed close to each −F atom while for −OH or $-NH_2$ group, two explicit water molecules were hydrogen-bonded so that three water molecules were used for molecules **1**, **3** and **4** while for molecule **2**, we included five water molecules. The number of solvent water molecules is chosen to be identical for all conformers of a molecule while the number of formed hydrogen bonds depends on the structure of each conformer. For molecules **3** and **4**, similar investigations are done with chloroform molecules as an explicit solvent. All geometry optimizations were performed by DFT with the dispersion-corrected S12g functional[83] and the cc-pVTZ basis set[84] in the NWChem software.[85] Geometry optimizations of single molecules were carried out in both the gas phase and in solution employing the conductor-like screening model (COSMO),[86,87] whereas

for clusters including explicit solvent molecules, geometries were only optimized in the gas phase. The reason for using different models and softwares for the geometry optimization and the property calculations is that we wanted to use the S12g functional in the geometry optimization. The S12g functional is essentially a modified PBE functional[88] with a Grimme D3 dispersion correction[89] that we have used in our previous work.[39,40] Since the calculated optical rotation is related to a pure enantiomeric structure, the experimental data were corrected for enantiomeric excess (ee) equal to 100%.

3. Results and Discussions

Optical rotations in the gas phase and in solution using different solvent methods as well as the experimental results, $[\alpha]_{\text{expt.}}$, are presented in Tables 1−3. $[\alpha]_{\text{m}}^{\text{PCM}}$ and $[\alpha]_{\text{m}}$ are the optical rotations for the isolated molecule with and without using PCM. $[\alpha]_{\text{mw}}$, in Tables 1 and 2, and $[\alpha]_{\text{mc}}$, in Table 3, denote the optical rotations in a solvation cluster of water and chloroform molecules, respectively, whereas $[\alpha]_{\text{mw}}^{\text{PCM}}$ and $[\alpha]_{\text{mc}}^{\text{PCM}}$ are their counterparts including also PCM. In addition, we give the optical rotations of the water (chloroform) molecules only, with and without employing PCM, $[\alpha]_{\text{w}}^{\text{PCM}}$ ($[\alpha]_{\text{c}}^{\text{PCM}}$) and $[\alpha]_{\text{w}}$ ($[\alpha]_{\text{c}}$) in Tables 1−3, implying an effect from the water (chloroform) molecules hydrogen-bonded to the chiral molecule which have a well-defined orientation.[56,57] The implicit solvent effects using PCM have been calculated for both water ($\varepsilon_{\text{static}} = 78.35$ and $\varepsilon_{\text{opt}} = 1.77$) and the solvent used in the experiments, that is, ethanol ($\varepsilon_{\text{static}} = 24.85$ and $\varepsilon_{\text{opt}} = 1.85$) for molecules containing the 1-naphthalene group and chloroform ($\varepsilon_{\text{static}} = 4.71$ and $\varepsilon_{\text{opt}} = 2.06$) for those containing the 4-(benzyloxy)phenyl group where $\varepsilon_{\text{static}}$ and ε_{opt} denote the static and optical dielectric constants, respectively. We find similar optical rotation results for both cases, because ε_{opt} of the solvents are close to each other, and therefore for molecules containing the 1-naphthalene group, we discuss only the results obtained for water although for compounds with the 4-(benzyloxy)phenyl group, results of both water and chloroform are presented in Tables 2 and 3, respectively. We

note that all PCM calculations are performed in the non-equilibrium regime and the atomic radii were determined from the universal force field (UFF).[90] In Tables 1−3, we present the relative energies with respect to the most stable structures with and without using PCM for isolated molecules, ΔE_m^{PCM} and ΔE_m, and solvation clusters, ΔE_{mw}^{PCM} and ΔE_{mw} (ΔE_{mc}^{PCM} and ΔE_{mc}), employing the CAM-B3LYP functional and the aug-cc-pVDZ basis set. In our previous work,[40] comparing theoretical and experimental results showed large absolute deviations and opposite optical rotation signs for the most stable conformers of some compounds with the 1-naphthalene group and the 4-(benzyloxy)phenyl group, respectively. Here, we investigate two representative molecules of each group whose results for molecules **1** and **2** are presented in Table 1 as well as for molecules **3** and **4** in Tables 2 and 3, employing water and chloroform as solvent, respectively. As indicated in Tables 1−3, both sign and magnitude of optical rotations may depend crucially on the conformation, which also have been demonstrated elsewhere.[39,40,55,91–98]

Figures 2−16 present the optimized structures for molecules **1**−**4** where Figures 2, 4, 6 and 9 display the optimized conformers according to their increasing gas phase energies. The optimized configurations of molecules **1**−**4** with water molecules are shown in Figures 3−11 whereas for molecules **3** and **4**, the optimized configurations with chloroform molecules are given in Figures 13−16. The conformers are labeled (a)−(d) for molecules **1** and **2** and (a)−(c) for molecules **3** and **4** where (a) denotes the most stable conformer in the gas phase for all cases. We have investigated conformations with and without internal hydrogen bonds for all molecules. In general, internal hydrogen bonds often result in stable conformers in the gas phase whereas structures without internal hydrogen bonds may be more stable when including an explicit solvent by forming hydrogen bonds with the surrounding solvent molecules.

Figures 2(a)−2(d) show four optimized conformers of molecule **1** in the gas phase where conformer (a) is the most stable structure. Conformers (a) and (b) are stabilized by an internal hydrogen bond $-OH\cdots F$ in contrast to conformers (c) and (d). Conformers (a)

Table 1: Specific optical rotations for different conformers of molecules 1 and 2 depicted in Figures 2−5 at $\lambda = 589$ nm. Relative energy with respect to the most stable conformer (a) with and without the PCM model, ΔE_m^{PCM} and $\Delta E_m = |E_{Con.} - E_{(a)}|$ (kJ mol^{-1}), calculated optical rotations in the gas phase and solvent using PCM, $[\alpha]_m$ and $[\alpha]_m^{PCM}$ (deg[dm g/cm^3]$^{-1}$), as well as experimental results, $[\alpha]_{expt.}$ (deg[dm g/cm^3]$^{-1}$). For structures with water molecules, relative energy and optical rotation are denoted by ΔE_{mw} (kJ mol^{-1}) and $[\alpha]_{mw}$ (deg[dm g/cm^3]$^{-1}$) while their counterparts including PCM are shown by ΔE_{mw}^{PCM} (kJ mol^{-1}) and $[\alpha]_{mw}^{PCM}$ (deg[dm g/cm^3]$^{-1}$), respectively. Also, the optical rotations of only the water configuration are given with and without the PCM model by $[\alpha]_w^{PCM}$ and $[\alpha]_w$.

n	Con.	molecule				molecule + water molecules				water molecules		
		ΔE_m	ΔE_m^{PCM}	$[\alpha]_m$	$[\alpha]_m^{PCM}$	ΔE_{mw}	ΔE_{mw}^{PCM}	$[\alpha]_{mw}$	$[\alpha]_{mw}^{PCM}$	$[\alpha]_w$	$[\alpha]_w^{PCM}$	$[\alpha]_{expt.}$
1	(a)	0	0	135.8	111.4	25.28	22.73	21.3	22.9	-13.1	-12.1	**59.4**
	(b)	5.91	4.81	-67.8	-66.2	38.65	27.21	-51.1	-40.0	0.8	1.6	**(EtOH)** [66]
	(c)	6.78	1.32	187.5	148.8	0	0	140.8	100.0	1.6	4.4	
	(d)	11.48	6.42	15.3	-13.0	5.07	6.24	53.8	-8.5	11.4	13.5	
2	(a)	0	0	-100.0	-70.9	20.60	17.19	-29.2	-42.6	1.6	0.1	**-12.8**
	(b)	4.01	0.94	-136.7	-92.3	0	0	-40.7	-44.7	8.6	14.6	**(EtOH)** [63]
	(c)	4.88	3.99	72.9	61.5	33.78	24.94	5.6	12.6	-5.6	-0.8	
	(d)	7.98	5.56	12.5	27.9	3.78	5.25	-2.3	8.3	6.4	9.7	

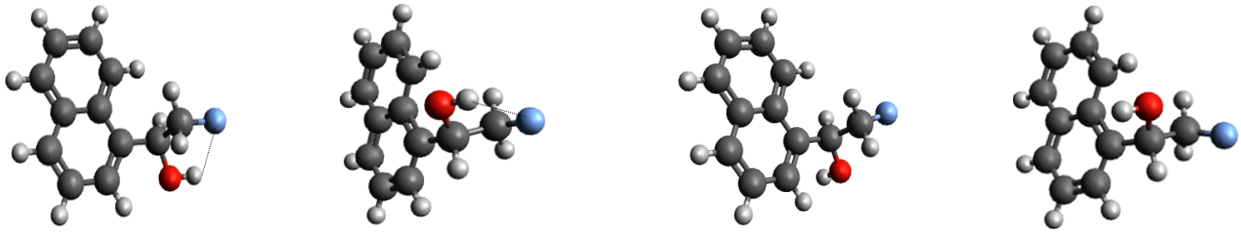

(a) (b) (c) (d)

Figure 2: Optimized conformers of molecule **1** ordered by increasing gas phase energies from (a) to (d). Hydrogen bonds are represented by " $\cdots$ ".

and (c) have a positive optical rotation sign (consistent with experiment) in both the gas phase and in the PCM model while the sign for conformers (b) and (d) is negative except for conformer (d) which is positive in the gas phase. Although the optical rotation magnitudes are reduced by using PCM for all conformers, the magnitudes are a factor of two to three times larger than the experimental result for conformers (a) and (c). Optimized structures of molecule **1** including three water molecules are given in Figures 3(a)−3(d). Conformers

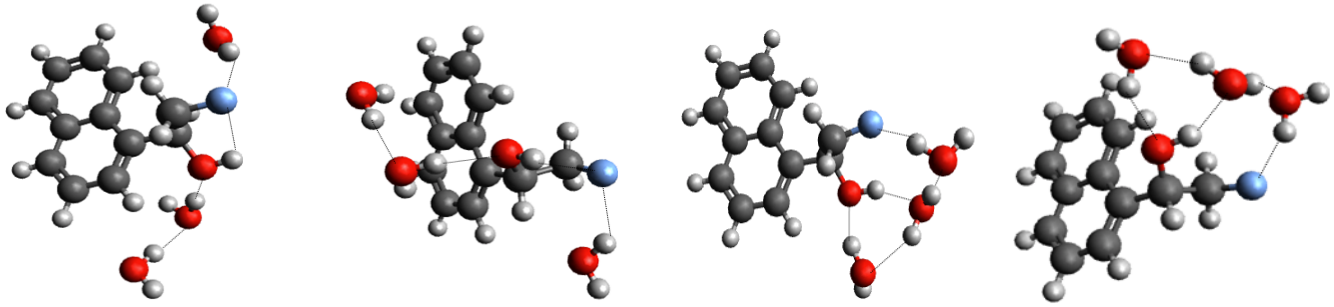

(a) (b) (c) (d)

Figure 3: Optimized conformers of molecule **1** with three extra water molecules where (a) to (d) correspond to the conformations in Figure 2. Hydrogen bonds are shown by " $\cdots$ ".

(c) and (d) (without internal hydrogen bonds) now become the most stable structures since they form more hydrogen bonds with the water molecules as compared to conformers (a) and (b). The optical rotation signs are consistent with the calculations without explicit water molecules. For the most stable conformer (c), the microsolvation model improves the optical rotation results compared to the experiment considerably. This method with and without PCM gives 100.0 and 140.8 deg[dm g/cm^3]$^{-1}$, respectively, as compared to the experimental result of 59.4 deg[dm g/cm^3]$^{-1}$. For conformer (d), $[\alpha]_{\mathrm{mw}}$ and $[\alpha]_{\mathrm{mw}}^{\mathrm{PCM}}$ are 53.8 and -8.5 deg[dm g/cm^3]$^{-1}$ where the latter is opposite to the experimental sign. The optical rotation of only water molecules for conformer (c), $[\alpha]_{\mathrm{w}}^{\mathrm{PCM}}$ (4.4 deg[dm g/cm^3]$^{-1}$), is small compared to the total optical rotation, $[\alpha]_{\mathrm{mw}}^{\mathrm{PCM}}$ (100.0 deg[dm g/cm^3]$^{-1}$), which indicates a small but significant contribution to the solvent effect. A proper sampling at the experimental temperature in a molecular dynamics simulation may give an appropriate distribution of conformers (c) and (d) in a solvent and thereby an $[\alpha]$ closer to experiment and is the suggested route to improve on these results.

Four optimized conformers of molecule **2** are given in Figures 4(a)−4(d). Conformers (a) and (c) have an internal hydrogen bond $-\mathrm{OH}\cdots\mathrm{F}$ in contrast to conformers (b) and (d). The calculations give a negative optical rotation sign for conformers (a) and (b), which is consistent with the experimental result, while conformers (c) and (d) have positive optical rotations. For conformers (a) and (b), the predicted magnitudes are considerably larger than

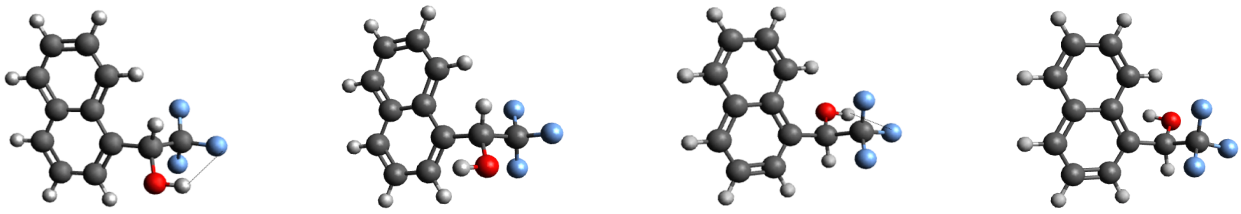

(a) (b) (c) (d)

Figure 4: Optimized conformers of molecule **2** ordered by increasing gas phase energies from (a) to (d). We show hydrogen bonds by " $\cdots$ ".

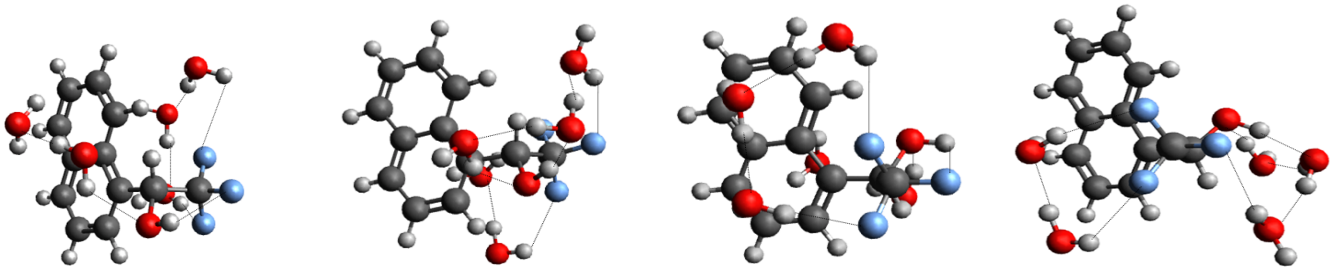

(a) (b) (c) (d)

Figure 5: Optimized conformers of molecule **2** with five extra water molecules where (a) to (d) correspond to the conformations in Figure 4. We label hydrogen bonds by " $\cdots$ ".

experiments. As for molecule **1**, PCM reduces the optical rotation magnitudes of conformers (a)-(c), but here the optical rotation for conformer (d) is increased by PCM as compared to the gas phase. In Figures 5(a)−5(d), we present the optimized configurations of molecule **2** surrounded by five water molecules. The most stable conformers are again those without internal hydrogen bonds i.e. conformers (b) and (d) which form more hydrogen bonds with the surrounding water molecules as compared to conformers (a) and (c). The only sign change for $[\alpha]_{\rm mw}$ is for conformer (d) which becomes negative (-2.3 deg[dm g/cm^3]$^{-1}$) consistent with experiment -12.8 deg[dm g/cm^3]$^{-1}$. The inclusion of water molecules reduces the optical rotation magnitudes for all conformers. For the lowest energy conformer (b) with explicit solvent molecules, $[\alpha]_{\rm mw}$ and $[\alpha]_{\rm mw}^{\rm PCM}$ are -40.7 and -44.7 deg[dm g/cm^3]$^{-1}$ which are in reasonable agreement with experiment. The optical rotation of only water molecules, $[\alpha]_{\rm w}^{\rm PCM}$, for conformer (b) is 14.6 deg[dm g/cm^3]$^{-1}$ again demonstrating that the contribution from a rigid solvation shell may be significant.

Figures 6(a)−6(c) display three optimized conformers for molecule **3** in the gas phase.

Table 2: Specific optical rotations for different conformers of molecules 3 and 4 depicted in Figures 6−11 at $\lambda = 589$ nm. Relative energy with respect to the most stable conformer (a) with and without the PCM model, ΔE_m^{PCM} and $\Delta E_m = |E_{Con.} - E_{(a)}|$ (kJ mol^{-1}), calculated optical rotations in the gas phase and solvent using PCM, $[\alpha]_m$ and $[\alpha]_m^{PCM}$ (deg[dm g/cm^3]$^{-1}$), as well as experimental results, $[\alpha]_{expt.}$ (deg[dm g/cm^3]$^{-1}$). For structures with three/four extra water molecules, relative energies and optical rotations are denoted by $\Delta E_{mw}/\Delta E_{mw'}$ (kJ mol^{-1}) and $[\alpha]_{mw}/[\alpha]_{mw'}$ (deg[dm g/cm^3]$^{-1}$) while their counterparts including PCM are shown by $\Delta E_{mw}^{PCM}/\Delta E_{mw'}^{PCM}$ (kJ mol^{-1}) and $[\alpha]_{mw}^{PCM}/[\alpha]_{mw'}^{PCM}$ (deg[dm g/cm^3]$^{-1}$), respectively. Also, the optical rotations of only the water configuration are given with and without the PCM model by $[\alpha]_w^{PCM}/[\alpha]_{w'}^{PCM}$ and $[\alpha]_w/[\alpha]_{w'}$.

n	Con.	molecule				molecule + water molecules				water molecules		
		ΔE_m	ΔE_m^{PCM}	$[\alpha]_m$	$[\alpha]_m^{PCM}$	ΔE_{mw}	ΔE_{mw}^{PCM}	$[\alpha]_{mw}$	$[\alpha]_{mw}^{PCM}$	$[\alpha]_w$	$[\alpha]_w^{PCM}$	$[\alpha]_{expt.}$
3	(a)	0	0	11.9	-73.7	39.28	33.99	23.0	8.8	-8.7	-8.7	**-34.9**
	(b)	0.37	1.57	140.1	101.5	38.80	34.39	109.4	75.9	-9.7	-9.7	**(CHCl3)** [64]
	(c)	7.31	1.53	-82.9	-128.5	0	0	96.9	77.2	35.6	24.2	
4	(a)	0	0	121.2	100.8	13.72	10.30	153.7	130.3	-10.4	-10.5	**-30.3**
	(b)	0.27	0.50	111.7	89.0	11.37	7.04	-11.3	-12.2	-11.6	-10.2	**(CHCl3)** [65]
	(c)	16.26	4.82	-111.4	-126.2	0	0	184.1	134.1	-11.6	-7.0	
						$\Delta E_{mw'}$	$\Delta E_{mw'}^{PCM}$	$[\alpha]_{mw'}$	$[\alpha]_{mw'}^{PCM}$	$[\alpha]_{w'}$	$[\alpha]_{w'}^{PCM}$	
3	(a)					43.85	39.16	-57.2	-64.3	-4.7	-4.0	
	(b)					43.07	39.07	24.9	-9.4	-11.1	-10.5	
	(c)					0	0	-54.9	-44.4	1.8	-4.4	
4	(a)					19.01	10.34	-13.7	-15.3	-7.9	-5.8	
	(b)					15.58	8.44	-58.5	-49.6	-7.0	-5.2	
	(c)					0	0	-85.0	-30.6	-8.3	-5.8	

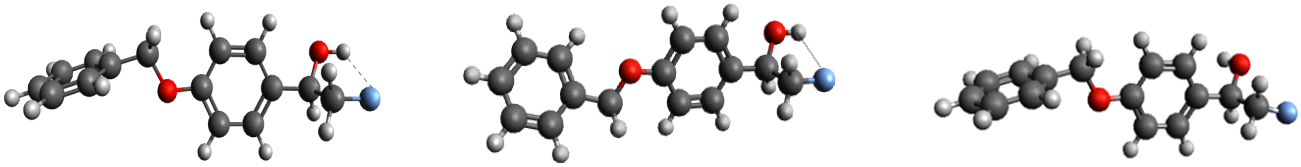

(a) (b) (c)

Figure 6: Optimized conformers of molecule **3** ordered by increasing gas phase energies from (a) to (c). We represent hydrogen bonds by "$\cdots$".

The structures of the two lowest minima (a) and (b) with close energies are stabilized by an internal $-OH\cdots F$ hydrogen bond in contrast to conformer (c). For $[\alpha]_m$, positive optical rotation signs are predicted for conformers (a) and (b) although their magnitudes are quite different. The calculation with PCM gives a negative optical rotation, consistent with

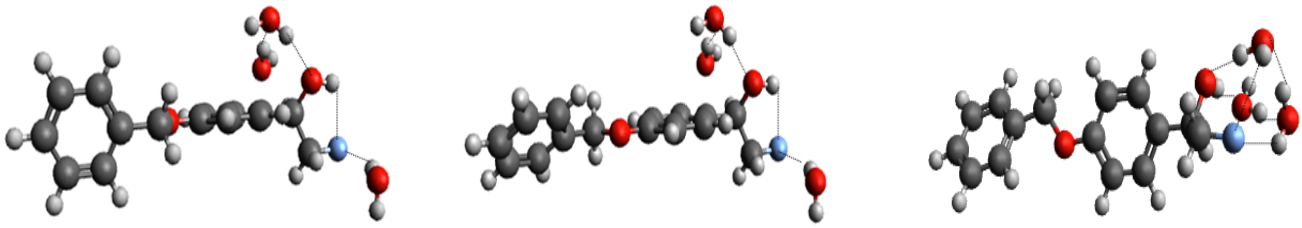

(a) (b) (c)

Figure 7: Optimized conformers of molecule **3** with three extra water molecules where (a) to (c) correspond to the conformations in Figure 6. Hydrogen bonds are indicated by " $\cdots$ ".

experiment, for conformer (a) while a positive rotation is predicted for conformer (b). For conformer (c), the optical rotation sign is negative. Using PCM, the magnitude of the optical rotation is reduced for conformer (b), while for conformers (a) and (c), the magnitudes increase. For molecules **3** and **4**, we evaluated both three and four water molecules, where the additional water molecule was placed on the ether oxygen to identify this effect separately. The optimized structures of molecule **3** with three water molecules are shown in Figures 7(a)−7(c). Conformation (c) (without the internal hydrogen bond) is now the most stable structure since, as for the previous molecules, it can form more hydrogen bonds to the water molecules. As in the gas phase, the energy of conformers (a) and (b) are rather similar. The microsolvation model predicts positive optical rotations for all configurations in contrast to experiment, -34.9 deg[dm g/cm^3]$^{-1}$ and the optical rotation magnitudes are reduced by the PCM model. The optical rotation for conformer (c), that in the gas phase had the same sign as experiment, has changed dramatically to a large positive value with the explicit solvation. Although $[\alpha]_{\mathrm{w}}^{\mathrm{PCM}}$ is negative and small in magnitude for conformers (a) and (b), it indicates a significant contribution of the chirality of only water molecules. For conformer (c), $[\alpha]_{\mathrm{w}}^{\mathrm{PCM}}$ is 24.2 deg[dm g/cm^3]$^{-1}$ which is a relatively large contribution to the total value, $[\alpha]_{\mathrm{mw}}^{\mathrm{PCM}}$=77.2 deg[dm g/cm^3]$^{-1}$.

We also investigated the optimized structures of molecule **3** with four water molecules, displayed in Figures 8(a)−8(c), where the extra water molecule is hydrogen-bonded to the ether oxygen atom in the benzyloxy group and the results are presented in Table 2. As for

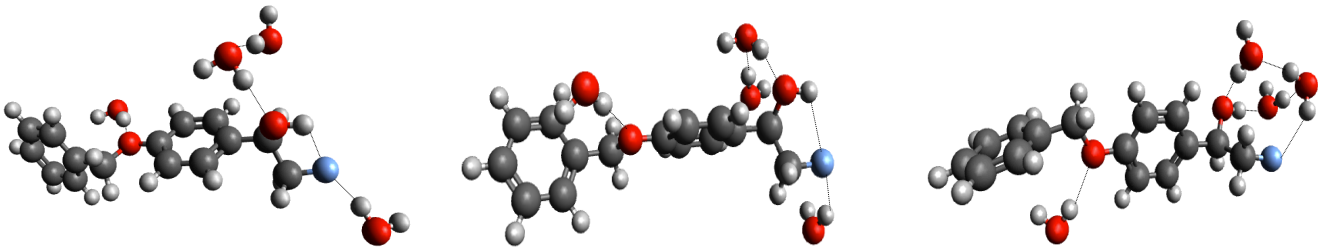

(a) (b) (c)

Figure 8: Optimized conformers of molecule **3** with four extra water molecules where (a) to (c) correspond to the conformations in Figure 6. Hydrogen bonds are indicated by " $\cdots$ ".

the structures in Figure 7 with three water molecules, conformers (a) and (b) have similar energies and conformer (c) is the most stable structure. However, the microsolvation model together with PCM predicts negative optical rotations for all configurations now consistent with the experimental data, -34.9 deg[dm g/cm^3]$^{-1}$. For conformer (c), $[\alpha]^{\mathrm{PCM}}_{\mathrm{mw}}$ is -44.4 deg[dm g/cm^3]$^{-1}$, which is in reasonable agreement with the experimental value of -34.9 deg[dm g/cm^3]$^{-1}$.

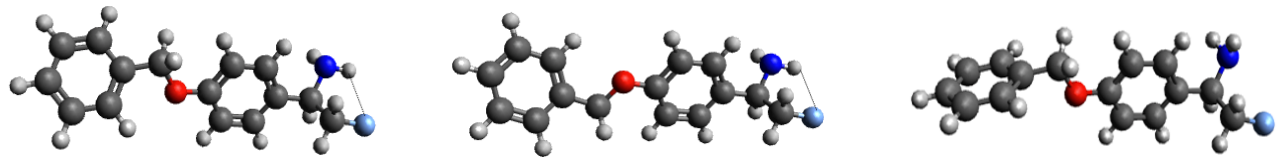

(a) (b) (c)

Figure 9: Optimized conformers of molecule **4** ordered by increasing gas phase energies from (a) to (c). Hydrogen bonds are denoted by " $\cdots$ ".

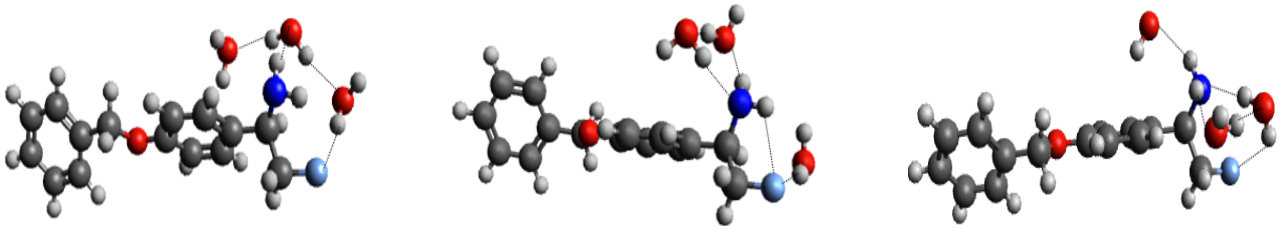

(a) (b) (c)

Figure 10: Optimized conformers of molecule **4** with three extra water molecules where (a) to (c) correspond to the conformations in Figure 9. Hydrogen bonds are denoted by " $\cdots$ ".

Three optimized conformers of molecule **4** in the gas phase are given in Figures 9(a)−9(c). These conformers are similar to those of molecule **3**, but molecule **4** has an $-NH_2$ group

instead of the −OH group in molecule **3**. Conformers (a) and (b) have an internal −NH$\cdots$F hydrogen bond in contrast to conformer (c). Conformers (a) and (b) are the most stable structures with similar energies and optical rotations with positive signs, whereas the experiment results in a negative optical rotation, -30.3 deg[dm g/cm^3]$^{-1}$. Conformer (c), with a higher energy in the gas phase, has a negative optical rotation consistent with experiment although with a larger magnitude. For conformers (a) and (b), PCM reduces the optical rotation magnitudes while for conformer (c), the magnitude increases using PCM. Figures 10(a)−10(c) show the optimized structures of molecule **4** with three extra water molecules. As for molecule **3**, conformer (c) is now the most stable conformer. Adding explicit water molecules, the optical rotation sign for structures (b) and (c) change so that for conformer (b), the negative sign predicted is consistent with the experiment while the sign of conformer (c) becomes contrary to the experiment. Comparing $[\alpha]_{\mathrm{mw}}^{\mathrm{PCM}}$ and $[\alpha]_{\mathrm{w}}^{\mathrm{PCM}}$ for conformer (c) (134.1 and -7.0 deg[dm g/cm^3]$^{-1}$, respectively) shows a relatively small contribution from the chirality of the solvent while for conformer (b), $[\alpha]_{\mathrm{mw}}^{\mathrm{PCM}}$ and $[\alpha]_{\mathrm{w}}^{\mathrm{PCM}}$ are close (-12.2 and -10.2 deg[dm g/cm^3]$^{-1}$) indicating a large relative contribution of the induced chirality of the ordered solvent.

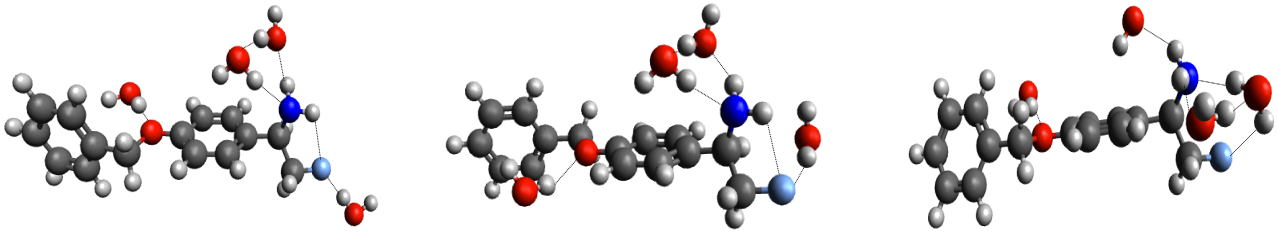

(a) (b) (c)

Figure 11: Optimized conformers of molecule **4** with four extra water molecules where (a) to (c) correspond to the conformations in Figure 9. Hydrogen bonds are denoted by " $\cdots$ ".

Figures 11(a)−11(c) show the optimized structures of molecule **4** with four explicit water molecules and the results are presented in Table 2. Here, conformer (c) is still the most stable conformer. Adding the fourth water molecule, the optical rotation signs turn to negative for all conformers consistent with the experimental result, -30.3 deg[dm g/cm^3]$^{-1}$. The

PCM model reduces the optical rotation magnitudes for conformers (b) and (c), while the magnitude of conformer (a) is increased slightly. For conformer (c), the microsolvation model with and without using PCM, $[\alpha]^{\mathrm{PCM}}_{\mathrm{mw'}}$ and $[\alpha]_{\mathrm{mw'}}$, gives -30.6 and -85.0 deg[dm g/cm^3]$^{-1}$.

Next, we investigate conformer (c) of molecules **3** and **4** in more detail because the optical rotation changes from a relatively large negative optical rotation to a large positive value by adding three explicit water molecules, while by adding one extra water molecule, the signs are reversed becoming consistent with experiments. First, we study the effect of hydrogen bonds between the solute and water molecules on the change of the optical rotation sign. For this purpose, we calculate the optical rotations for the chiral molecules optimized in solvation clusters but excluding the water molecules in the optical rotation calculation for the cases of both three, $[\alpha]_{\mathrm{mw\text{-}w}}$, and four, $[\alpha]_{\mathrm{mw'\text{-}w'}}$, explicit water molecules. For conformer (c) of molecule **3**, $[\alpha]_{\mathrm{mw\text{-}w}}$ and $[\alpha]_{\mathrm{mw'\text{-}w'}}$ are 105.7 and -72.3 deg[dm g/cm^3]$^{-1}$, respectively, which are similar to the optical rotations obtained with water molecules. For conformer (c) of molecule **4**, we get 138.6 and -133.8 deg[dm g/cm^3]$^{-1}$ for $[\alpha]_{\mathrm{mw\text{-}w}}$ and $[\alpha]_{\mathrm{mw'\text{-}w'}}$, respectively, similar to the values with water molecules.

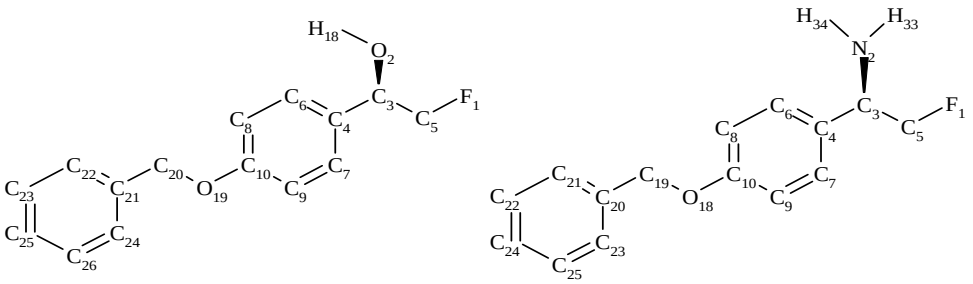

(*R*)-3 **(*R*)-4**

Figure 12: The structures of molecules **3** and **4**.

Secondly, we compare the dihedral angles for conformer (c) of molecules **3** and **4** (shown in Figure 12) when adding three or four water molecules, respectively, for finding shifts in the geometry of the solute molecule by adding water molecules and thereby reasons of the optical rotation sign reversal. The most important changes are found in the dihedral angles of $\tau(\mathrm{O_{19}C_{20}C_{21}C_{24}})$ and $\tau(\mathrm{O_{18}C_{19}C_{20}C_{23}})$ in the 4-(benzyloxy)phenyl group for molecules **3** and

4, respectively. For molecule **3**, the dihedral angle $\tau(O_{19}C_{20}C_{21}C_{24})$ is 88.4° in the gas phase which decreases to 41.4° by adding three explicit water molecules, whereas the magnitude increases to 98.5° for four water molecules and becomes similar to the dihedral angle in the gas phase. The dihedral angle $\tau(O_{18}C_{19}C_{20}C_{23})$ in the 4-(benzyloxy)phenyl group is 100.2° for conformer (c) of molecule **4**, which as for molecule **3**, the magnitude is reduced for three water molecules to 48.6° whereas for four explicit water molecules the dihedral angle is 98.5° again similar to the dihedral angle in the gas phase. In addition, for conformer (c) of molecules **3** and **4**, the gas phase optical rotations, $[\alpha]_{\mathrm{m}}$, are -82.9 and -111.4 deg[dm g/cm^3]$^{-1}$ close to the corresponding $[\alpha]_{\mathrm{mw'\text{-}w'}}$ results i.e -72.3 and -133.8 deg[dm g/cm^3]$^{-1}$, respectively, whereas the $[\alpha]_{\mathrm{mw\text{-}w}}$ values are given 105.7 and 138.6 deg[dm g/cm^3]$^{-1}$, respectively. Therefore, it is the effect of this dihedral angle that has to be modelled accurately in a computational model of optical rotation for these molecules.

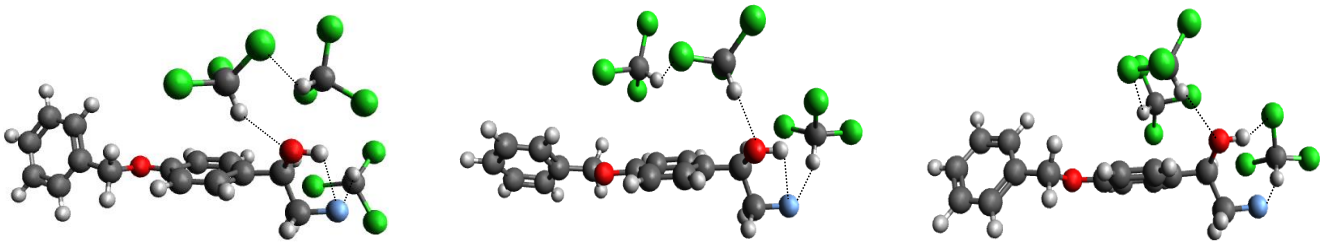

(a) (b) (c)

Figure 13: Optimized conformers of molecule **3** with three extra chloroform molecules where (a) to (c) correspond to the conformations in Figure 6. Hydrogen bonds are indicated by "$\cdots$".

As for water, chloroform also form hydrogen bonds to the solute.[99–101] Chloroform is, however, a quite different solvent than water and it would be interesting to investigate the difference between water and chloroform in a microsolvation model. Table 3 presents the optical rotation results for molecules **3** and **4** using chloroform as a solvent. As mentioned earlier, the optical rotations for the isolated molecules using PCM, $[\alpha]_{\mathrm{m}}^{\mathrm{PCM}}$, are similar to the results given in Table 2 where water was used as the implicit solvent. The optimized structures of molecule **3** with three explicit chloroform molecules are shown in Figures 13(a)−13(c). As for

Table 3: Specific optical rotations for different conformers of molecules 3 and 4 depicted in Figures 6, 9, and 13−16 at $\lambda = 589$ nm. Relative energy with respect to the most stable conformer (a) with and without the PCM model, ΔE_m^{PCM} and $\Delta E_m = |E_{Con.} - E_{(a)}|$ (kJ mol^{-1}), calculated optical rotations in the gas phase and solvent using PCM, $[\alpha]_m$ and $[\alpha]_m^{PCM}$ (deg[dm g/cm^3]$^{-1}$), as well as experimental results, $[\alpha]_{expt.}$ (deg[dm g/cm^3]$^{-1}$). For structures with three/four extra chloroform molecules, relative energies and optical rotations are denoted by $\Delta E_{mc}/\Delta E_{mc'}$ (kJ mol^{-1}) and $[\alpha]_{mc}/[\alpha]_{mc'}$ (deg[dm g/cm^3]$^{-1}$) while their counterparts including PCM are shown by $\Delta E_{mc}^{PCM}/\Delta E_{mc'}^{PCM}$ (kJ mol^{-1}) and $[\alpha]_{mc}^{PCM}/[\alpha]_{mc'}^{PCM}$ (deg[dm g/cm^3]$^{-1}$), respectively. Also, the optical rotations of only the chloroform configuration are given with and without the PCM model by $[\alpha]_c^{PCM}/[\alpha]_{c'}^{PCM}$ and $[\alpha]_c/[\alpha]_{c'}$.

n	Con.	molecule				molecule + CHCl3 molecules				CHCl3 molecules		
		ΔE_m	ΔE_m^{PCM}	$[\alpha]_m$	$[\alpha]_m^{PCM}$	ΔE_{mc}	ΔE_{mc}^{PCM}	$[\alpha]_{mc}$	$[\alpha]_{mc}^{PCM}$	$[\alpha]_c$	$[\alpha]_c^{PCM}$	$[\alpha]_{expt.}$
3	(a)	0	0	11.9	-43.3	1.97	2.35	11.7	-3.7	-52.3	-23.4	**-34.9**
	(b)	0.37	1.27	140.1	95.2	0.26	1.43	20.6	24.2	23.3	17.2	**(CHCl3)** [64]
	(c)	7.31	3.20	-82.9	-125.9	0	0	-78.1	-81.2	39.7	28.5	
4	(a)	0	0	121.2	93.2	5.15	4.84	-61.2	-83.5	-29.6	-5.5	**-30.3**
	(b)	0.27	0.52	111.7	80.1	4.68	5.52	-10.6	-6.3	18.1	20.7	**(CHCl3)** [65]
	(c)	16.26	8.79	-111.4	-114.3	0	0	-25.2	-5.5	-5.1	2.7	
						$\Delta E_{mc'}$	$\Delta E_{mc'}^{PCM}$	$[\alpha]_{mc'}$	$[\alpha]_{mc'}^{PCM}$	$[\alpha]_{c'}$	$[\alpha]_{c'}^{PCM}$	
3	(a)					5.90	3.81	-3.7	-23.3	-44.0	-15.9	
	(b)					3.77	2.28	-79.2	-52.7	-60.9	-26.7	
	(c)					0	0	-35.5	-15.3	29.2	1.8	
4	(a)					7.92	7.72	-31.7	-17.6	20.1	7.5	
	(b)					4.43	5.18	-35.2	-42.4	24.8	31.8	
	(c)					0	0	-95.1	-66.5	-8.9	2.7	

three water molecules in Figure 7, conformer (c) is the most stable structure. Similar to the gas phase results, the microsolvation model predicts positive optical rotations for conformers (a) and (b) whereas the optical rotation sign is negative for conformer (c) consistent with the experiment. The calculations with PCM give negative optical rotations for conformers (a) and (c) while a positive rotation is predicted for conformer (b). Using PCM, the optical rotation magnitude is reduced for conformer (a) whereas the magnitudes are increased for conformers (b) and (c). $[\alpha]_{mc}^{PCM}$ is -81.2 deg[dm g/cm^3]$^{-1}$ for conformer (c) compared to experiment which is -34.9 deg[dm g/cm^3]$^{-1}$. The optical rotation of only chloroform molecules, $[\alpha]_c^{PCM}$, is positive and relatively large in magnitude, 28.5 deg[dm g/cm^3]$^{-1}$, for conformer

(c) which indicates that the contribution from a rigid solvation shell is significant also for chloroform.

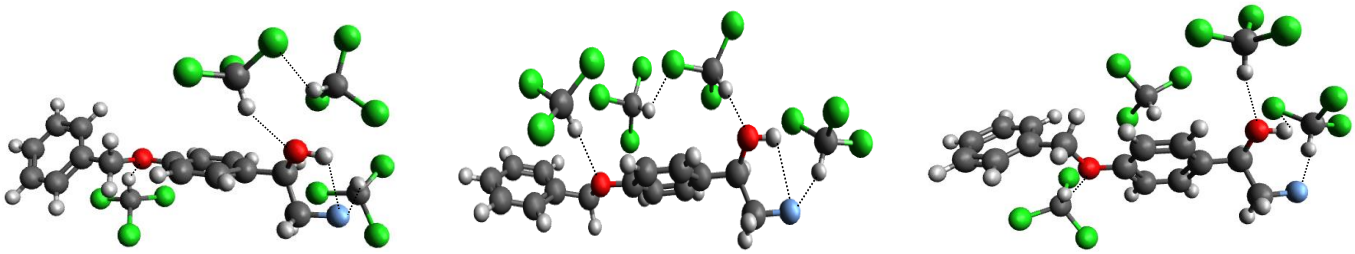

(a) (b) (c)

Figure 14: Optimized conformers of molecule **3** with four extra chloroform molecules where (a) to (c) correspond to the conformations in Figure 6. Hydrogen bonds are indicated by "...".

Figures 14(a)−14(c) show the optimized structures of molecule **3** with four chloroform molecules where again conformer (c) is the most stable structure. As for the structures with four explicit water molecules in Figure 8, negative optical rotations are predicted for all configurations, consistent with the experiment. The PCM model reduces the optical rotation magnitudes for conformers (b) and (c), whereas the magnitude of conformer (a) is increased. For conformer (c), the microsolvation model with and without PCM gives -15.3 and -35.5 deg[dm g/cm^3]$^{-1}$ for $[\alpha]^{\mathrm{PCM}}_{\mathrm{mc'}}$ and $[\alpha]_{\mathrm{mc'}}$, respectively, where the experimental result was reported as -34.9 deg[dm g/cm^3]$^{-1}$. Compared to $[\alpha]^{\mathrm{PCM}}_{\mathrm{mc'}}$, the optical rotation of only chloroform molecules for conformer (c), $[\alpha]^{\mathrm{PCM}}_{\mathrm{c'}}$, is 1.8 deg[dm g/cm^3]$^{-1}$ which indicates a small but significant contribution to the solvent effect.

The optimized structures of molecule **4** with three chloroform molecules are given in Figures 15(a)−15(c). As for molecule **3**, conformer (c) is the most stable structure. Adding explicit chloroform molecules, unlike the case of three water molecules, negative optical rotations are predicted for all configurations consistent with the experimental result, -30.3 deg[dm g/cm^3]$^{-1}$. For conformer (a), PCM increases the magnitude of the optical rotation (-83.5 deg[dm g/cm^3]$^{-1}$) whereas the magnitudes are reduced in conformers (b) and (c) to relatively small values of -6.3 and -5.5 deg[dm g/cm^3]$^{-1}$, respectively. $[\alpha]^{\mathrm{PCM}}_{\mathrm{mc}}$ and $[\alpha]^{\mathrm{PCM}}_{\mathrm{c}}$ for

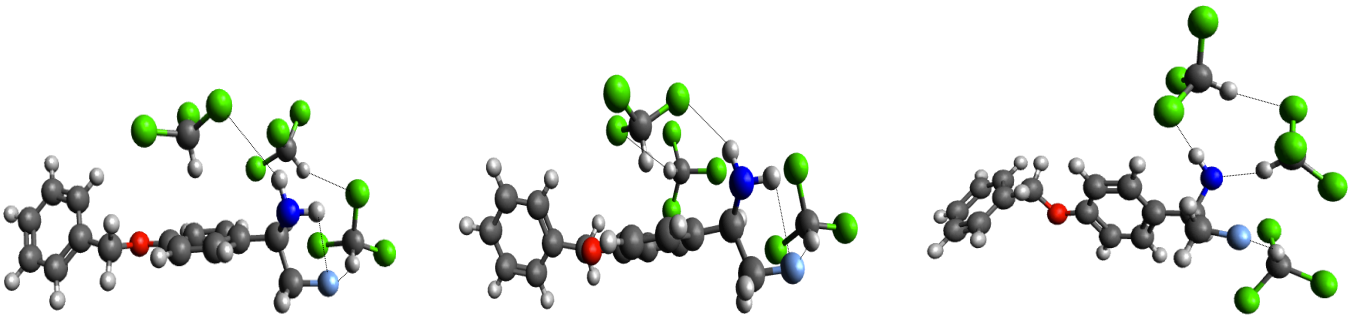

(a) (b) (c)

Figure 15: Optimized conformers of molecule **4** with three extra chloroform molecules where (a) to (c) correspond to the conformations in Figure 6. Hydrogen bonds are indicated by "...".

conformer (c) are -5.5 and 2.7 deg[dm g/cm^3]$^{-1}$, indicating a relatively small contribution from the chirality of the solvent whereas for conformer (b), comparing $[\alpha]_{\mathrm{mc}}^{\mathrm{PCM}}$ and $[\alpha]_{\mathrm{c}}^{\mathrm{PCM}}$ (-6.3 and 20.7 deg[dm g/cm^3]$^{-1}$) shows a large relative contribution by the induced chirality of only chloroform molecules.

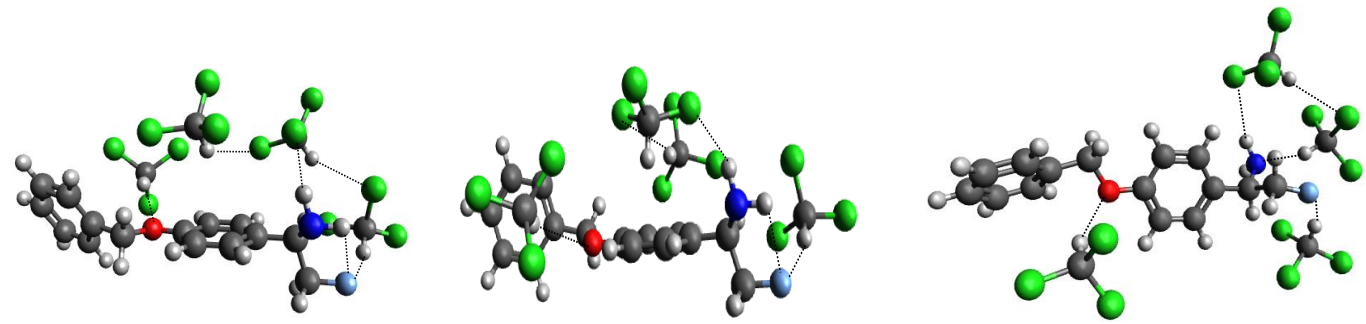

(a) (b) (c)

Figure 16: Optimized conformers of molecule **4** with three extra chloroform molecules where (a) to (c) correspond to the conformations in Figure 9. Hydrogen bonds are indicated by "...".

We also investigate the optimized structures of molecule **4** with four chloroform molecules, shown in Figures 16(a)−16(c). Conformer (c) is still the most stable conformer. As for three explicit chloroform molecules, negative optical rotations are predicted for all configurations consistent with experiment, -30.0 deg[dm g/cm^3]$^{-1}$. Using PCM, the optical rotation magnitude is reduced for conformer (a), whereas the PCM model increases the magnitude of the optical rotations for conformers (b) and (c). The microsolvation model with and without

using PCM, $[\alpha]^{\mathrm{PCM}}_{\mathrm{mc'}}$ and $[\alpha]_{\mathrm{mc'}}$, predicts -66.5 and -95.1 deg[dm g/cm^3]$^{-1}$ for conformer (c). The optical rotations of only chloroform molecules, $[\alpha]^{\mathrm{PCM}}_{\mathrm{c'}}$ and $[\alpha]_{\mathrm{c'}}$, are obtained -8.9 and 2.7 deg[dm g/cm^3]$^{-1}$ for conformer (c), indicating a relatively small contribution from the chirality of the solvent.

In contrast to water, the optical rotation sign for conformer (c) of molecules **3** and **4** remains negative by adding three or four explicit chloroform molecules. Analogous calculations to water are performed for the cases of three, $[\alpha]_{\mathrm{mc\text{-}c}}$, and four, $[\alpha]_{\mathrm{mc'\text{-}c'}}$, explicit chloroform molecules for conformer (c) of molecules **3** and **4**. $[\alpha]_{\mathrm{mc\text{-}c}}$ and $[\alpha]_{\mathrm{mc'\text{-}c'}}$ are -124.4 and -71.1 deg[dm g/cm^3]$^{-1}$, respectively, for conformer (c) of molecule **3** which are similar to the optical rotations with chloroform molecules. For conformer (c) of molecule **4**, -8.8 and -245.4 deg[dm g/cm^3]$^{-1}$ are obtained for $[\alpha]_{\mathrm{mc\text{-}c}}$ and $[\alpha]_{\mathrm{mc'\text{-}c'}}$, respectively, with the same optical rotation signs using chloroform molecules.

Similar investigations for dihedral angles are carried out for the cases of clusters including three or four explicit chloroform molecules where the sign of the optical rotation remains negative which is consistent with experiments. In the case of chloroform molecules, for conformer (c) of molecule **3**, the dihedral angle $\tau(\mathrm{O_{19}C_{20}C_{21}C_{24}})$ in the 4-(benzyloxy)phenyl group is 111.5° and 109.5° for three and four chloroform molecules, respectively, which is relatively similar to the dihedral angle in the gas phase, 88.4°. The dihedral angle $\tau(\mathrm{O_{18}C_{19}C_{20}C_{23}})$ for conformer (c) of molecule **4** is 83.9° for three chloroform molecules and the magnitude is increased for four chloroform molecules to 126.0° where the dihedral angle in the gas phase is 100.2°. Therefore, for both molecules **3** and **4**, the dihedral angles in the 4-(benzyloxy)phenyl group remain almost unchanged for chloroform molecules compared to the gas phase dihedral angles, and in contrast to adding water molecules, so that the same optical rotation sign is obtained in the different cases. For conformer (c) of molecule **3**, $[\alpha]_{\mathrm{mc\text{-}c}}$ and $[\alpha]_{\mathrm{mc'\text{-}c'}}$ are -124.4 and -71.1 deg[dm g/cm^3]$^{-1}$, respectively, where the gas phase optical rotation, $[\alpha]_{\mathrm{m}}$, is -82.9 deg[dm g/cm^3]$^{-1}$. $[\alpha]_{\mathrm{mc\text{-}c}}$ and $[\alpha]_{\mathrm{mc'\text{-}c'}}$ are found -8.8 and -245.4 deg[dm g/cm^3]$^{-1}$ for conformer (c) of molecule **4** where $[\alpha]_{\mathrm{m}}$ is obtained -111.4 deg[dm g/cm^3]$^{-1}$. Comparing Ta-

bles 2 and 3, the energy differences, ΔE, between the conformations are considerably smaller when chloroform is added. Although it is the same conformation that has the lowest energy when adding water or chloroform, the other conformations are thus expected to have a much larger weight in the averaged optical rotation in chloroform as compared to water.

The results presented here indicate which factors that are important to get the correct optical rotation by studying model systems, and thus providing some important insights regarding these molecules. If one in contrast would like to get optical rotation values very close to experiment, a multitude of aspects need to be addressed in more detail. Perhaps most importantly, one should sample configurations from molecular dynamics simulations, but it is likely that thousands of configurations per molecule is needed,[102] but the number depends strongly on the property and the molecule. A Boltzmann averaging over the few data provided here would not be sufficient. The quality of the force field is crucial in these simulations, and in this case a validation of the force field for the dihedral angle of importance would be crucial. A black-box approach without this prior information about these molecules may lead to poor results if not this dihedral is described accurately in the force field. To construct accurate force fields for molecules with dihedral degrees of freedom is by no means a trivial task.[103] Furthermore, since we have relatively high energy barriers between the different conformations, the molecular dynamics sampling scheme needs to include a method that efficiently samples the relative importance of different local minima as for example adding an umbrella potential. In addition, vibrational averaging is also important for optical rotation,[104] and for molecules with low-frequency modes a path-integral approach is suitable.[105,106] Finally, using water molecules to model the hydrogen bonds instead of the solvents used in the experiments is a further simplification. Using ethanol, for example, would lead to further aspects to be addressed as for example the sampling of the dihedral angle of the ethanol molecules.

4. Conclusions

The optical rotation of several conformers of four fluorinated molecules containing the 1-naphthalene or 4-(benzyloxy)phenyl group at the stereocenter have been investigated by employing the CAM-B3LYP functional in both the gas phase and in an aqueous environment at $\lambda = 589$ nm. The selection of molecules has been motivated by our recent theoretical study for the optical rotation of 45 fluorinated alcohols, amines, amides and esters[40] where molecules containing the 1-naphthalene group showed the largest absolute deviations with respect to experiments, and opposite optical rotation signs in comparison to experiment were obtained in the gas phase for molecules containing the 4-(benzyloxy)phenyl group. We have employed the PCM model and explicit solute-solvent interactions combined with PCM. In general, PCM only gives smaller optical rotation magnitudes and almost the same signs as compared to the gas phase results.

For molecules **1** and **2**, the reduction of absolute deviations between computational and experimental results show improvements in the optical rotations by considering both implicit and explicit contributions from an aqueous solvent. For the most stable conformers in an explicit solvent, the microsolvation approach with water molecules reduces the values of optical rotation so that this method provides optical rotations relatively close to experiments. For the second category of compounds, molecules **3** and **4**, the explicit solvent method was investigated for two cases with three and four water molecules as well as three and four chloroform molecules. Adding three water molecules, the optical rotation signs were opposite to experiments for all conformers except for conformer (b) of molecule **4**. However, the fourth extra water molecule hydrogen-bonded to the ether oxygen atom in the 4-(benzyloxy)phenyl group changed the optical rotation signs for all conformers of molecules **3** and **4**, now consistent with the experiments. In the case of three chloroform molecules, the sign of the optical rotations were consistent with the experiments expect for conformer (b) of molecule **3**. As for water molecules, the optical rotation signs for all conformers became consistent with experiments by adding four explicit chloroform molecules. The major changes in the structure

of conformer (c) of both molecules after adding three water molecules can be linked to a large dihedral angle reduction in the 4-(benzyloxy)phenyl group while four extra water molecules increase this dihedral angle back close to the gas phase value. For the situation of chloroform molecules, the change of the dihedral angle is small in the 4-(benzyloxy)phenyl group for both three and four explicit chloroform molecules so that this dihedral angle remains close to the gas phase value for conformer (c) of both molecules **3** and **4**. Our studies for both groups of molecules indicate that the microsolvation model in conjunction with PCM gives results consistent with experiments.

Supporting Information

Optimized geometries of both isolated molecules and solvation clusters in the gas phase in xyz coordinates.

Acknowledgement

A grant of computer time is acknowledged from the NOTUR project (account 2920k) at the Norwegian Research Council. H.K. acknowledges financial support from the FP7-PEOPLE-2013-IOF funding scheme (project No. 625321).

References

(1) Crabbé, P. *Optical Rotatory Dispersion and Circular Dichroism in Organic Chemistry*; Holden-Day series in physical techniques in chemistry; Holden-Day: San Francisco, 1965.

(2) Mason, S. F. *Molecular Optical Activity and the Chiral Discriminations*; Cambridge University Press: Cambridge, United Kingdom, 1982.

(3) Sokolov, V. I. *Chirality and Optical Activity in Organometallic Compounds*; Gordon and Breach Science Publishers: New York, 1990.

(4) Collins, A. N.; Sheldrake, G. N.; Crosby, J. *Chirality in Industry: The Commercial Manufacture and Applications of Optically Active Compounds*; John Wiley & Sons: New York, 1992.

(5) Berova, N., Nakanishi, K., Woody, R. W., Eds. *Circular Dichroism: Principles and Applications*, 2nd ed.; Wiley-VCH: New York, 2000.

(6) Reddy, I. K., Mehvar, R., Eds. *Chirality in Drug Design and Development*; Marcel Dekker: New York, 2004.

(7) Corradini, R.; Sforza, S.; Tedeschi, T.; Marchelli, R. Chirality as a Tool in Nucleic Acid Recognition: Principles and Relevance in Biotechnology and in Medicinal Chemistry. *Chirality* **2007**, *19*, 269–294.

(8) Amouri, H.; Gruselle, M. *Chirality in Transition Metal Chemistry: Molecules, Supramolecular Assemblies and Materials*; John Wiley & Sons: Chichester, United Kingdom, 2008.

(9) Amabilino, D. B. *Chirality at the Nanoscale*; WILEY-VCH Verlag GmbH: Weinheim, Germany, 2009.

(10) Ladd, M. F. C. *Structure Determination by X-ray Crystallography*, 2nd ed.; Plenum Press: New York, 1985.

(11) Eliel, E. L.; Wilen, S. H. *Stereochemistry of Organic Compounds*; John Wiley & Sons: New York, 1994.

(12) Polavarapu, P. L.; Chakraborty, D. K. Absolute Stereochemistry of Chiral Molecules from Ab Initio Theoretical and Experimental Molecular Optical Rotations. *J. Am. Chem. Soc.* **1998**, *120*, 6160–6164.

(13) Stephens, P. J.; Devlin, F. J.; Cheeseman, J. R.; Frisch, M. J.; Rosini, C. Determination of Absolute Configuration Using Optical Rotation Calculated Using Density Functional Theory. *Org. Lett.* **2002**, *4*, 4595–4598.

(14) McCann, D. M.; Stephens, P. J.; Cheeseman, J. R. Determination of Absolute Configuration Using Density Functional Theory Calculation of Optical Rotation: Chiral Alkanes. *J. Org. Chem.* **2004**, *69*, 8709–8717.

(15) Giorgio, E.; Viglione, R. G.; Zanasi, R.; Rosini, C. Ab Initio Calculation of Optical Rotatory Dispersion (ORD) Curves: A Simple and Reliable Approach to the Assignment of the Molecular Absolute Configuration. *J. Am. Chem. Soc.* **2004**, *126*, 12968–12976.

(16) McCann, D. M.; Stephens, P. J. Determination of Absolute Configuration Using Density Functional Theory Calculations of Optical Rotation and Electronic Circular Dichroism: Chiral Alkenes. *J. Org. Chem.* **2006**, *71*, 6074–6098.

(17) McCurdy, C. W.; Rescigno, T. N.; Yeager, D. L.; McKoy, V. In *Methods of Electronic Structure Theory*; Schaefer III, H. F., Ed.; Plenum Press: New York, 1977.

(18) Bouman, T. D.; Hansen, Aa. E. Ab Initio Calculations of Oscillator and Rotatory Strengths in the Random-Phase Approximation: Twisted Mono-Olefins. *J. Chem. Phys.* **1977**, *66*, 3460–3467.

(19) Oddershede, J. Polarization Propagator Calculations. *Adv. Quant. Chem.* **1978**, *11*, 275–352.

(20) Hansen, Aa. E.; Bouman, T. D. Natural Chiraoptical Spectroscopy: Theory and Computations. *Adv. Chem. Phys.* **1980**, *44*, 545–644.

(21) Bouman, T. D.; Hansen, Aa. E.; Voigt, B.; Rettrup, S. Large-Scale RPA Calculations of Chiroptical Properties of Organic Molecules: Program RPAC. *Int. J. Quant. Chem.* **1983**, *23*, 595–611.

(22) Hansen, Aa. E.; Bouman, T. D. Optical Activity of Monoolefins: RPA Calculations and Extraction of the Mechanisms in Kirkwood's Theory. Application to (-)-trans-Cyclooctene and 3(3R)-3-Methylcyclopentene. *J. Am. Chem. Soc.* **1985**, *107*, 4828–4839.

(23) Polavarapu, P. L. Ab Initio Molecular Optical Rotations and Absolute Configurations. *Mol. Phys.* **1997**, *91*, 551–554.

(24) Cheeseman, J. R.; Frisch, M. J.; Devlin, F. J.; Stephens, P. J. Hartree-Fock and Density Functional Theory ab Initio Calculation of Optical Rotation Using GIAOs: Basis Set Dependence. *J. Phys. Chem. A* **2000**, *104*, 1039–1046.

(25) Stephens, P. J.; Devlin, F. J.; Cheeseman, J. R.; Frisch, M. J. Calculation of Optical Rotation Using Density Functional Theory. *J. Phys. Chem. A* **2001**, *105*, 5356–5371.

(26) Grimme, S. Calculation of Frequency Dependent Optical Rotation Using Density Functional Response Theory. *Chem. Phys. Lett.* **2001**, *339*, 380–388.

(27) Grimme, S.; Furche, F.; Ahlrichs, R. An Improved Method for Density Functional Calculations of the Frequency-Dependent Optical Rotation. *Chem. Phys. Lett.* **2002**, *361*, 321–328.

(28) Ruud, K.; Helgaker, T. Optical Rotation Studied by Density-Functional and Coupled-Cluster Methods. *Chem. Phys. Lett.* **2002**, *352*, 533–539.

(29) Autschbach, J.; Patchkovskii, S.; Ziegler, T.; van Gisbergen, S. J. A.; Baerends, E. J. Chiroptical Properties from Time-Dependent Density Functional Theory. II. Optical Rotations of Small to Medium Sized Organic Molecules. *J. Chem. Phys.* **2002**, *117*, 581–592.

(30) Stephens, P. J.; McCann, D. M.; Cheeseman, J. R.; Frisch, M. J. Determination of Absolute Configurations of Chiral Molecules Using ab Initio Time-Dependent Den-

sity Functional Theory Calculations of Optical Rotation: How Reliable Are Absolute Configurations Obtained for Molecules with Small Rotations? *Chirality* **2005**, *17*, S52–S64.

(31) Pedersen, T. B.; Kongsted, J.; Crawford, T. D.; Ruud, K. On the Importance of Vibrational Contributions to Small-Angle Optical Rotation: Fluoro-Oxirane in Gas Phase and Solution. *J. Chem. Phys.* **2009**, *130*, 034310.

(32) Baranowska, A.; Łaczkowski, K. Z.; Sadlej, A. J. Model Studies of the Optical Rotation, and Theoretical Determination of its Sign for β-Pinene and trans-Pinane. *J. Comput. Chem.* **2010**, *31*, 1176–1181.

(33) Srebro, M.; Govind, N.; de Jong, W. A.; Autschbach, J. Optical Rotation Calculated with Time-Dependent Density Functional Theory: The OR45 Benchmark. *J. Phys. Chem. A* **2011**, *115*, 10930–10949.

(34) Mach, T. J.; Crawford, T. D. Basis Set Dependence of Coupled Cluster Optical Rotation Computations. *J. Phys. Chem. A* **2011**, *115*, 10045–10051.

(35) Wiberg, K. B.; Caricato, M.; Wang, Y.-G.; Vaccaro, P. H. Towards the Accurate and Efficient Calculation of Optical Rotatory Dispersion Using Augmented Minimal Basis Sets. *Chirality* **2013**, *25*, 606–616.

(36) Baranowska-Łaczkowska, A.; Łaczkowski, K. Z. The ORP Basis Set Designed for Optical Rotation Calculations. *J. Comput. Chem.* **2013**, *34*, 2006–2013.

(37) Lahiri, P.; Wiberg, K. B.; Vaccaro, P. H. Intrinsic Optical Activity and Large-Amplitude Displacement: Conformational Flexibility in (R)-Glycidyl Methyl Ether. *J. Phys. Chem. A* **2015**, *119*, 8311–8327.

(38) Haghdani, S.; Åstrand, P.-O.; Koch, H. Optical Rotation from Coupled Cluster and

Density Functional Theory: The Role of Basis Set Convergence. *J. Chem. Theory Comput.* **2016**, *12*, 535–548.

(39) Haghdani, S.; Gautun, O. R.; Koch, H.; Åstrand, P.-O. Optical Rotation Calculations for a Set of Pyrrole Compounds. *J. Phys. Chem. A* **2016**, *120*, 7351–7360.

(40) Haghdani, S.; Hoff, B. H.; Koch, H.; Åstrand, P.-O. Optical Rotation Calculations for Fluorinated Alcohols, Amines, Amides and Esters. *J. Phys. Chem. A* **2016**, *120*, 7973–7986.

(41) Ruud, K.; Stephens, P. J.; Devlin, F. J.; Taylor, P. R.; Cheeseman, J. R.; Frisch, M. J. Coupled-Cluster Calculations of Optical Rotation. *Chem. Phys. Lett.* **2003**, *373*, 606–614.

(42) Pedersen, T. B.; Sánchez de Merás, A. M. J.; Koch, H. Polarizability and Optical Rotation Calculated from the Approximate Coupled Cluster Singles and Doubles CC2 Linear Response Theory Using Cholesky Decompositions. *J. Chem. Phys.* **2004**, *120*, 8887–8897.

(43) Pedersen, T. B.; Koch, H.; Boman, L.; Sánchez de Merás, A. M. J. Origin Invariant Calculation of Optical Rotation without Recource to London Orbitals. *Chem. Phys. Lett.* **2004**, *393*, 319–326.

(44) Tam, M. C.; Russ, N. J.; Crawford, T. D. Coupled Cluster Calculations of Optical Rotatory Dispersion of (S)-Methyloxirane. *J. Chem. Phys.* **2004**, *121*, 3550–3557.

(45) Crawford, T. D.; Owens, L. S.; Tam, M. C.; Schreiner, P. R.; Koch, H. *Ab Initio* Calculation of Optical Rotation in (P)-(+)-[4]Triangulane. *J. Am. Chem. Soc.* **2005**, *127*, 1368–1369.

(46) Crawford, T. D. *Ab Initio* Calculation of Molecular Chiroptical Properties. *Theor. Chem. Acc.* **2006**, *115*, 227–245.

(47) Tam, M. C.; Crawford, T. D. *Ab Initio* Determination of Optical Rotatory Dispersion in the Conformationally Flexible Molecule (R)-Epichlorohydrin. *J. Phys. Chem. A* **2006**, *110*, 2290–2298.

(48) Kowalczyk, T. D.; Abrams, M. L.; Crawford, T. D. *Ab Initio* Optical Rotatory Dispersion and Electronic Circular Dichroism Spectra of (S)-2-Chloropropionitrile. *J. Phys. Chem. A* **2006**, *110*, 7649–7654.

(49) Kumata, Y.; Furukawa, J.; Fueno, T. The Effect of Solvents on the Optical Rotation of Propylene Oxide. *Bull. Chem. Soc (Jpn)* **1970**, *43*, 3920–3921.

(50) Cancès, E.; Mennucci, B.; Tomasi, J. A New Integral Equation Formalism for the Polarizable Continuum Model: Theoretical Background and Applications to Isotropic and Anisotropic Dielectrics. *J. Chem. Phys.* **1997**, *107*, 3032–3041.

(51) Cancès, E.; Mennucci, B. New Applications of Integral Equations Methods for Solvation Continuum Models: Ionic Solutions and Liquid Crystals. *J. Mater. Chem.* **1998**, *23*, 309–326.

(52) Tomasi, J.; Mennucci, B.; Cammi, R. Quantum Mechanical Continuum Solvation Models. *Chem. Rev.* **2005**, *105*, 2999–3093.

(53) Mennucci, B. Continuum Solvation Models: What Else Can We Learn from Them? *J. Phys. Chem. Lett.* **2010**, *1*, 1666–1674.

(54) Kongsted, J.; Ruud, K. Solvent Effects on Zero-Point Vibrational Corrections to Optical Rotations and Nuclear Magnetic Resonance Shielding Constants. *Chem. Phys. Lett.* **2008**, *451*, 226–232.

(55) Wilson, S. M.; Wiberg, K. B.; Murphy, M. J.; Vaccaro, P. H. The Effects of Conformation and Solvation on Optical Rotation: Substituted Epoxides. *Chirality* **2008**, *20*, 357–369.

(56) Mukhopadhyay, P.; Zuber, G.; Goldsmith, M.-R.; Wipf, P.; Beratan, D. N. Solvent Effect on Optical Rotation: A Case Study of Methyloxirane in Water. *ChemPhysChem* **2006**, *7*, 2483–2486.

(57) Mukhopadhyay, P.; Zuber, G.; Wipf, P.; Beratan, D. Contribution of a Solute's Chiral Solvent Imprint to Optical Rotation. *Angew. Chem. Int. Ed.* **2007**, *46*, 6450–6452.

(58) Kundrat, M. D.; Autschbach, J. Ab Initio and Density Functional Theory Modeling of the Chiroptical Response of Glycine and Alanine in Solution Using Explicit Solvation and Molecular Dynamics. *J. Chem. Theory Comput.* **2008**, *4*, 1902–1914.

(59) Kundrat, M. D.; Autschbach, J. Modeling of the Chiroptical Response of Chiral Amino Acids in Solution Using Explicit Solvation and Molecular Dynamics. *J. Chem. Theory Comput.* **2009**, *5*, 1051–1060.

(60) Mennucci, B.; Cappelli, C.; Cammi, R.; Tomasi, J. Modeling Solvent Effects on Chiroptical Properties. *Chirality* **2011**, *23*, 717–729.

(61) Pikulska, A.; Hopmann, K. H.; Bloino, J.; Pecul, M. Circular Dichroism and Optical Rotation of Lactamide and 2-Aminopropanol in Aqueous Solution. *J. Phys. Chem. B* **2013**, *117*, 5136–5147.

(62) Cappelli, C. Integrated QM/polarizable MM/continuum approaches to model chiroptical properties of strongly interacting solute–solvent systems. *Int. J. Quant. Chem.* **2016**, *116*, 1532–1542.

(63) Xu, Q.; Zhou, H.; Geng, X.; Chen, P. Nonenzymatic Kinetic Resolution of Racemic 2,2,2-Trifluoro-1-Aryl Ethanol via Enantioselective Acylation. *Tetrahedron* **2009**, *65*, 2232–2238.

(64) Lystvet, S. M.; Hoff, B. H.; Anthonsen, T.; Jacobsen, E. E. Chemoenzymatic Synthe-

sis of Enantiopure 1-Phenyl-2-Haloethanols and Their Esters. *Biocatal. Biotransform* **2010**, *28*, 272–278.

(65) Thvedt, T. H. K.; Fuglseth, E.; Sundby, E.; Hoff, B. H. Enantioenriched 1-aryl-2-Fluoroethylamines. Efficient Lipase-Catalysed Resolution and Limitations to the Mitsunobu Inversion Protocol. *Tetrahedron* **2010**, *66*, 6733–6743.

(66) Slungård, S. V.; Krakeli, T.-A.; Thvedt, T. H. K.; Fuglseth, E.; Sundby, E.; Hoff, B. H. Investigation into the Enantioselection Mechanism of Ruthenium-Arene-Diamine Transfer Hydrogenation Catalysts Using Fluorinated Substrates. *Tetrahedron* **2011**, *67*, 5642–5650.

(67) Yanai, T.; Tew, D. P.; Handy, N. C. A New Hybrid Exchange-Correlation Functional Using the Coulomb-Attenuating Method (CAM-B3LYP). *Chem. Phys. Lett.* **2004**, *393*, 51–57.

(68) Dunning Jr., T. H. Gaussian Basis Sets for Use in Correlated Molecular Calculations. I. The Atoms Boron through Neon and Hydrogen. *J. Chem. Phys.* **1989**, *90*, 1007–1023.

(69) Kendall, R. A.; Dunning Jr., T. H.; Harrison, R. J. Electron Affinities of the First-Row Atoms Revisited. Systematic Basis Sets and Wave Functions. *J. Chem. Phys.* **1992**, *96*, 6796–6806.

(70) Woon, D. E.; Dunning Jr., T. H. Gaussian Basis Sets for Use in Correlated Molecular Calculations. IV. Calculation of Static Electrical Response Properties. *J. Chem. Phys.* **1994**, *100*, 2975–2988.

(71) Wilson, A. K.; van Mourik, T.; Dunning, Jr., T. H. Gaussian Basis Sets for Use in Correlated Molecular Calculations. VI. Sextuple zeta Correlation Consistent Basis Sets for Boron through Neon. *J. Mol. Struct. (THEOCHEM)* **1997**, *388*, 339–349.

(72) Peach, M. J. G.; Cohen, A. J.; Tozer, D. J. Influence of Coulomb-Attenuation on Exchange-Correlation Functional Quality. *Phys. Chem. Chem. Phys.* **2006**, *8*, 4543–4549.

(73) Pecul, M. Conformational Structures and Optical Rotation of Serine and Cysteine. *Chem. Phys. Lett.* **2006**, *418*, 1–10.

(74) Srebro, M.; Autschbach, J. Tuned Range-Separated Time-Dependent Density Functional Theory Applied to Optical Rotation. *J. Chem. Theory Comput.* **2012**, *8*, 245–256.

(75) Runge, E.; Gross, E. K. U. Density-Functional Theory for Time-Dependent Systems. *Phys. Rev. Lett.* **1984**, *52*, 997–1000.

(76) Gross, E. K. U.; Dobson, J. F.; Petersilka, M. Density Functional Theory of Time-Dependent Phenomena. *Top. Curr. Chem.* **1996**, *181*, 81–172.

(77) Marques, M. A. L.; Gross, E. K. U. Time-Dependent Density Functional Theory. *Ann. Rev. Phys. Chem.* **2004**, *55*, 427–455.

(78) Frisch, M. J.; Trucks, G. W.; Schlegel, H. B.; Scuseria, G. E.; Robb, M. A.; Cheeseman, J. R.; Scalmani, G.; Barone, V.; Mennucci, B.; Petersson, G. A. et al. Gaussian09 Revision E.01. Gaussian Inc. Wallingford CT 2009.

(79) London, F. Théorie Quantique des Courants Interatomiques dans les Combinaisons Aromatiques. *J. Phys. Radium* **1937**, *8*, 397–409.

(80) Ditchfield, R. Self-Consistent Perturbation Theory of Diamagnetism. *Mol. Phys.* **1974**, *27*, 789–807.

(81) Helgaker, T.; Jørgensen, P. An Electronic Hamiltonian for Origin Independent Calculations of Magnetic Properties. *J. Chem. Phys.* **1991**, *95*, 2595–2601.

(82) Purvis, G. D.; Bartlett, R. J. A Full Coupled-Cluster Singles and Doubles Model: The Inclusion of Disconnected Triples. *J. Chem. Phys.* **1982**, *76*, 1910–1918.

(83) Swart, M. A New Family of Hybrid Density Functionals. *Chem. Phys. Lett.* **2013**, *580*, 166–171.

(84) van Lenthe, E.; Baerends, E. J. Optimized Slater-Type Basis Sets for the Elements 1-118. *J. Comput. Chem.* **2003**, *24*, 1142–1156.

(85) Valiev, M.; Bylaska, E. J.; Govind, N.; Kowalski, K.; Straatsma, T. P.; van Dam, H. J. J.; Wang, D.; Nieplocha, J.; Apra, E.; Windus, T. L. et al. NWChem: A Comprehensive and Scalable Open-Source Solution for Large Scale Molecular Simulations. *Comput. Phys. Commun.* **2010**, *181*, 1477–1489.

(86) Klamt, A.; Schüürmann, G. COSMO: A New Approach to Dielectric Screening in Solvents with Explicit Expressions for the Screening Energy and its Gradient. *J. Chem. Soc., Perkin Trans. 2* **1993**, 799–805.

(87) Hornig, M.; Klamt, A. COSMO$frag$: A Novel Tool for High-Throughput ADME Property Prediction and Similarity Screening Based on Quantum Chemistry. *J. Chem. Inf. Model.* **2005**, *45*, 1169–1177.

(88) Perdew, J. P.; Burke, K.; Ernzerhof, M. Generalized Gradient Approximation Made Simple. *Phys. Rev. Lett.* **1996**, *77*, 3865–3868.

(89) Grimme, S.; Antony, J.; Ehrlich, S.; Krieg, H. A Consistent and Accurate Ab Initio Parametrization of Density Functional Dispersion Correction (DFT-D) for the 94 Elements H-Pu. *J. Chem. Phys.* **2010**, *132*, 154104.

(90) Rappé, A. K.; Casewit, C. J.; Colwell, K. S.; Goddard III, W. A.; Skiff, W. M. UFF, a Full Periodic Table Force Field for Molecular Mechanics and Molecular Dynamics Simulations. *J. Am. Chem. Soc.* **1992**, *114*, 10024–10035.

(91) Wiberg, K. B.; Vaccaro, P. H.; Cheeseman, J. R. Conformational Effects on Optical Rotation. 3-Substituted 1-Butenes. *J. Am. Chem. Soc.* **2003**, *125*, 1888–1896.

(92) Pecul, M.; Ruud, K.; Rizzo, A.; Helgaker, T. Conformational Effects on the Optical Rotation of Alanine and Proline. *J. Phys. Chem. A* **2004**, *108*, 4269–4276.

(93) Marchesan, D.; Coriani, S.; Forzato, C.; Nitti, P.; Pitacco, G.; Ruud, K. Optical Rotation Calculation of a Highly Flexible Molecule: The Case of Paraconic Acid. *J. Phys. Chem. A* **2005**, *109*, 1449–1453.

(94) Coriani, S.; Baranowska, A.; Ferrighi, L.; Forzato, C.; Marchesan, D.; Nitti, P.; Pitacco, G.; Rizzo, A.; Ruud, K. Solvent Effects on the Conformational Distribution and Optical Rotation of Methyl Paraconic Acids and Esters. *Chirality* **2006**, *18*, 357–369.

(95) Tam, M. C.; Abrams, M. L.; Crawford, T. D. Chiroptical Properties of (R)-3-Chloro-1-butene and (R)-2-Chlorobutane. *J. Phys. Chem. A* **2007**, *111*, 11232–11241.

(96) Lahiri, P.; Wiberg, K. B.; Vaccaro, P. H. A Tale of Two Carenes: Intrinsic Optical Activity and Large-Amplitude Nuclear Displacement. *J. Phys. Chem. A* **2012**, *116*, 9516–9533.

(97) Lahiri, P.; Wiberg, K. B.; Vaccaro, P. H. Intrinsic Optical Activity and Conformational Flexibility: The Role of Size-Dependent Ring Morphology in Model Cycloketones. *J. Phys. Chem. A* **2013**, *117*, 12382–12400.

(98) Caricato, M. Conformational Effects on Specific Rotation: A Theoretical Study Based on the $\tilde{S}_k$ Method. *J. Phys. Chem. A* **2015**, *119*, 8303–8310.

(99) Campbell, A. N.; Kartzmark, E. M. The Energy of Hydrogen Bonding in the System: Acetone-Chloroform. *Can. J. Chem.* **1960**, *38*, 652–655.

(100) Choi, K.; Tedder, D. W. Molecular Interactions in Chloroform-Diluent Mixtures. *AIChE J.* **1997**, *43*, 196–211.

(101) Goutev, N.; Matsuura, H. Hydrogen Bonding in Chloroform Solutions of Ethylenedioxy Ethers. Spectroscopic Evidence of Bifurcated Hydrogen Bonds. *J. Phys. Chem. A* **2001**, *105*, 4741–4748.

(102) Osted, A.; Kongsted, J.; Mikkelsen, K. V.; Åstrand, P.-O.; Christiansen, O. Statistically Mechanically Averaged Molecular Properties of Liquid Water Calculated Using the Combined Coupled Cluster/Molecular Dynamics Method. *J. Chem. Phys.* **2006**, *124*, 124503.

(103) Engkvist, O.; Åstrand, P.-O.; Karlström, G. Intermolecular Potential for the 1,2-Dimethoxyethane-Water Complex. *J. Phys. Chem.* **1996**, *100*, 6950–6957.

(104) Ruud, K.; Taylor, P. R.; Åstrand, P.-O. Zero-Point Vibrational Effects on Optical Rotation. *Chem. Phys. Lett.* **2001**, *337*, 217–223.

(105) Böhm, M. C.; Schulte, J.; Ramírez, R. Nuclear Quantum Effects in Calculated NMR Shieldings of Ethylene; a Feynmann Path Integral - Ab Initio Study. *Chem. Phys. Lett.* **2000**, *332*, 117–124.

(106) Dračinský, M.; Bouř, P.; Hodgkinson, P. Temperature Dependence of NMR Parameters Calculated from Path Integral Molecular Dynamics Simulations. *J. Chem. Theory Comput.* **2016**, *12*, 968–973.

Graphical TOC Entry